Title

Comparison of gas analyzers for eddy covariance: Effects of analyzer type and spectral corrections on fluxes

Authors

Polonik, P

Chan, WS

Billesbach, DP

et al.

Publication Date

2019-07-01

DOI

10.1016/j.agrformet.2019.02.010

Peer reviewed

Comparison of gas analyzers for eddy covariance: Effects of analyzer type and spectral corrections on fluxes

P. Polonika,*[,1], W.S. Chan[a], D.P. Billesbach[b], G. Burba[c,b], J. Li[c], A. Nottrott[d], I. Bogoev[e], B. Conrad[e], S.C. Biraud[a]

[a] Lawrence Berkeley National Laboratory, Berkeley, CA, USA [b] University of Nebraska, Lincoln, NE, USA [c] LI-COR Biosciences, Lincoln, NE, USA [d] Picarro Inc., Santa Clara, CA, USA [e] Campbell Scientific, Logan, UT, USA

*Corresponding author. E-mail address: ppolonik@ucsd.edu (P. Polonik).

[1] Now at: Scripps Institution of Oceanography, University of California at San Diego, La Jolla, CA, USA.

Abstract

The eddy covariance technique (EC) is used at hundreds of field sites worldwide to measure trace gas exchange between the surface and the atmosphere. Data quality and correction methods for EC have been studied empirically and theoretically for many years. The recent development of new gas analyzers has led to an increase in technological options for users. Open-path (no inlet tube) and closed-path (long inlet tube) sensors have been used for a long time, whereas enclosed-path (short inlet tube) sensors are relatively new. We tested the comparability of fluxes calculated from five different gas analyzers including two open-path (LI-7500 A from LI-COR, IRGASON from Campbell), two enclosed-path (CPEC200 from Campbell, LI-7200 from LI-COR), and one closedpath (2311-f from Picarro) analyzers, which were all located on a single tower at an irrigated alfalfa field in Davis, CA. To effectively compare sensors with different tube characteristics we used three different spectral correction methods. We found that all sensors, regardless of type, can be used to measure fluxes if appropriate corrections are applied and quality control measures are taken. However, the comparability strongly depended on the gas (CO_2 or H_2O) and the correction method. Average differences were below 4% for CO_2 fluxes using any spectral correction method, but for H_2O average differences were between 4% and 13% for the different methods. The magnitude of corrections also varied strongly, especially for water vapor fluxes. This study does not identify the best sensor, but rather weighs the benefits and difficulties of each sensor and sensor type. Our findings show that enclosed and closed-path gas analyzers that measure water vapor with inlet tubes experience large high frequency attenuation and should be corrected with empirical correction methods. This information presented here about different the diverse sensors be considered by investigators when choosing a sensor for a site or when analyzing EC measurements from multiple sites.

Keywords: Eddy covariance, Carbon dioxide, Water vapor, Gas analyzer, Spectral correction, Frequency loss, Data quality

1. Introduction

Eddy covariance (EC), a micrometeorological technique, is widely used to measure the exchange of momentum, mass, and energy between the land surface and the atmosphere (Aubinet et al., 2012). The FLUXNET database, which aggregates global EC data, has more than 900 registered sites over a wide range of climate zones, terrains, and land uses (Baldocchi et al., 2001; Pastorello et al., 2017). EC requires high-frequency (typically 10 Hz or faster) measurements of vertical wind speed and a scalar, which are typically collected using three dimensional sonic anemometers sampling the horizontal and vertical wind components (u, v, and w), and gas analyzers sampling scalar gas concentrations (e.g., carbon dioxide (CO_2), water vapor (H_2O)). The surface fluxes, F_c, are calculated using:

$$F_c = \rho \overline{w'c'} \quad (1)$$

where ρ is the density of air, w' and c' are the deviations over time of the vertical wind speed and the scalar quantity from their respective means during the averaging period (typically 30 min) as denoted by the overbar. Temporal averaging requires invoking Taylor's hypothesis, which states that turbulent eddies are transported unchanged by the mean flow. The impact of this assumption on fluxes was explored in Cheng et al. (2017). There are several types of gas analyzers currently available that measure gas concentrations at frequencies suitable for EC. These sensor types can be differentiated by the route that the air takes before reaching the analyzer: "open-path", "closed-path", and "enclosed-path" sensors. In an open-path system, the analyzer is exposed to the air and gases are measured directly with minimal disturbance, while in a closed-path system the air is first drawn through a tube and sampled in a controlled cell within the gas analyzer. An enclosed-path system attempts to combine the benefits of an open-path gas analyzer and a closed-path system by utilizing fast temperature and pressure measurements of the sampled air in the cell, and a shorter tube (< 1 m) to minimize the air's residence time in the tube (Burba et al., 2010, 2012). Fast temperature measurements can also be avoided if the temperature fluctuations are sufficiently attenuated by the system (Sargent, 2015). Comparisons of open-path sensors to enclosed-path sensors (Clement et al., 2009; Burba et al., 2010; Nakai et al., 2011; Novick et al., 2013; Metzger et al., 2016) and closed-path sensors (Haslwanter et al., 2009), have shown promising agreement.

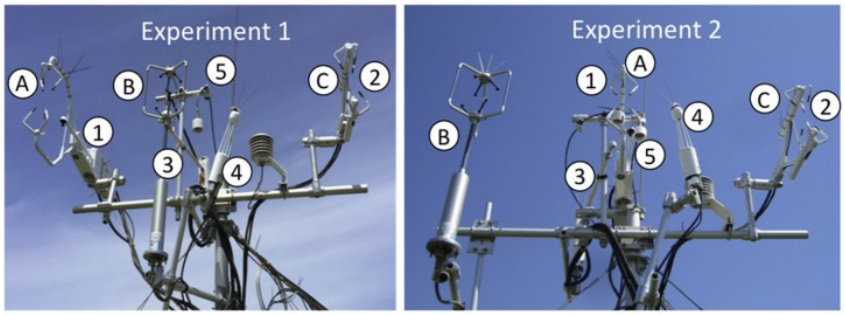

Fig. 1. Tower setup for the two study periods: experiment 1 (left) and experiment 2 (right). The five gas analyzers are labeled with numbers and the three sonic anemometers are labeled with letters (A: CSAT3A; B: Gill R3-50; C: IRGASON). Details about each instruments can be found in Table 1.

All gas analyzers and sonic anemometers used for EC act as low-pass filters. Attenuation of high-frequency signal leads to a bias in the variance and covariance of the gas concentration and wind speed measurements, and subsequently introduces a bias in fluxes, because of a few key sources including:

- Friction along the inner tube wall (Leuning and Moncrieff, 1990; Lenschow and Raupach, 1991) or adhesion of gas molecules to the tube itself, particularly for H_2O (Massman and Ibrom, 2008; Runkle et al., 2012). This attenuation has been shown to increase with tube age (Mammarella et al., 2009). The covariance loss due to tube attention is not applicable for open-path sensors.
- Time delay due to intake tube and electronics or data collection timing that, when uncorrected, lead to a covariance loss for all types of anemometers and gas sensors. These sources can be particularly significant for the systems with long intake tubes.
- Measurement of distorted flows by the sonic anemometer due to structures located close to the anemometer path (Dyer, 1981; Wyngaard, 1981, 1988; Frank et al., 2013, 2016; Horst et al., 2015, 2016; Grare et al., 2016; Huq et al., 2017). The erroneous loss or gain in the covariance due to various types of flow distortion in the anemometer (transducer shadowing, support arms, nearby sensors and structures, etc.) applies to all sensors, and strongly depends on instrument design and installation in relation to surrounding instruments and structures.
- Sensor time response leading to an ability of the sensor to respond fast enough to small fluctuations contributing to the flux (Moore, 1986; Horst, 2000). This source applies to a small degree to openpath sensors and is more often an issue with closed-path sensors.
- Volume and path averaging and physical separation between the sonic anemometer and gas analyzer that leads to undersampling of variance and/or covariance signals from small eddies (Moore, 1986).

- Other low-pass filters such as sensor response mismatch, digital sampling, and digital noise (Moore, 1986; Finnigan et al., 2003). These are generally small compared to other sources of frequency loss.

The differences between open and closed-path sensors can introduce large uncertainties in ecosystem studies. Mauder and Foken (2006) found that application of corrections can substantially improve energy balance closure, and Ueyama et al. (2012) found differences in gross primary productivity using open versus closed-path sensors even after sensor-appropriate processing options were applied.

Some of the causes of flux attenuation can be corrected in postprocessing (Moore, 1986; Leuning and Moncrieff, 1990; Leuning and King, 1992; Massman, 2000; Ibrom et al., 2007a; Massman and Ibrom, 2008) or minimized via instrument selection, setup, and deployment considerations (Lee and Black, 1994; Leuning and Judd, 1996; Horst and Lenschow, 2009). Processing corrections can be analytic (i.e. derived directly from theory) or empirical (i.e. calculated from collected data). Tube effects are known to cause high-frequency signal loss, but there are also several benefits associated with a gas analyzer that is not directly exposed to the atmosphere. Unlike open-path sensors, closed and enclosed-path sensors can function in foggy and rainy conditions without being physically obstructed. They also require much smaller density corrections (Leuning and Judd, 1996; Ibrom et al., 2007b) and are not subject to sensor heating corrections (Burba et al., 2008) because the air is analyzed in a controlled cell rather than directly in the atmosphere.

In this manuscript, five gas analyzers were evaluated side-by-side in an agricultural field (Fig. 1, Table 1). These were the open-path LI7500 A (LI-COR, Lincoln, NE, USA), and the open-path IRGASON (Campbell Scientific, Logan, UT, USA); enclosed-path CPEC200 (Campbell Scientific), and enclosed-path LI-7200 (LI-COR); closed-path 2311-f (Picarro Inc., Santa Clara, CA, USA). We present some of the observed differences between sensors as well as some of the benefits and difficulties unique to each sensor. The Picarro cavity ring-down spectroscopy (CRDS) analyzer employs a near-infrared laser source to quantify gas species concentration in a closed cell by measuring the time it takes for the gas sample to attenuate a given amount of input light energy (i.e. attenuation rate) (Crosson, 2008). The other infrared gas analyzers (IRGAs) in this experiment quantify gas species concentration by directly measuring the attenuation magnitude of the input light source caused by the gas sample.

Although smaller scale sensor comparisons have been conducted, this work, in close participation of each respective instrument manufacturer, sought to rigorously evaluate EC available gas analyzers to provide a resource for the flux community. Our unique dataset from five gas analyzers allowed us to test the comparability of measurements from the different available analyzer types and the effectiveness of some common spectral correction methods.

We show which corrections are most applicable to a given situation (e.g., sensor types, gases, etc.) and present the magnitude of each correction. In order to evaluate fluxes calculated from each gas analyzer, a detailed investigation of spectral correction methods was conducted. We applied two commonly used frequency corrections (Massman, 2000; Fratini et al., 2012) and a purely empirical correction based on similarity theory and the ratio of gas and sonic temperature cospectra (i.e. direct method). The information provided here is critical for both the EC practitioners who deploy instrumentation and conduct data processing routines, as well as for EC data users who should be aware of the potential uncertainties introduced by these decisions. The latter point is particularly relevant in the AmeriFlux network where sites may have different sensors and apply different (if any) spectral corrections.

Table 1
Specifications for the eddy covariance systems located on the tower. The anemometers are (A) CSAT3A, (B) Gill R3-50, (C) IRGASON. Sensor separation (x,y,z) is positive if the gas analyzer is East, North, and above the sonic anemometer.

Model [System] (#)	CPEC200 [EC155] (1)	IRGASON (2)	LI-7200 (3)	LI-7500A (4)	2311-f (5)
Manufacturer	Campbell Sci.	Campbell Sci.	LI-COR	LI-COR	Picarro
Spectroscopic method	Infrared	Infrared	Infrared	Infrared	Cavity ring-down laser absorption
Gas species	ρ_c, ρ_v, X_c, X_v	ρ_c, ρ_v	ρ_c, ρ_v, X_c, X_v	ρ_c, ρ_v	X_c, X_v,X_{CH4}
Sample path	Closed, heated short inlet	Open	Closed, short inlet	Open	Closed
Inlet (L x D) [cm]	58.4 × 0.27	N/A	60 × 0.533	N/A	850 × 0.432
Flow rate [L/min]	7	N/A	15	N/A	6
Anemometer exp1 (x,y,z separation [cm])	A (0,15,-6),	C(0,0,0),	B (-6,14,-6)	B (27,8,-20)	B (10,28,2)
Anemometer exp2	A (0,15,-6)	C(0,0,0),	A (-3,24,-1)	A (14,13,-10)	A (10,28,6)

2. Materials and methods

2.1. Study site

All instruments were deployed on a single 4 m tripod at the edge of an irrigated alfalfa field in Davis, California (38.5385 °N, 121.7767 °W). The field dimensions were about 100 m by 200 m. The alfalfa was harvested once per month during the growing season, typically near the beginning of the month. During each harvest cycle, the alfalfa grew to approximately 1 m height, with most of the growth occurring in the last two weeks of each cycle. Measurements were made between April 7th and October 6th, 2015. Temperatures were often 20-35°C during the day and 10-15°C at night. Most days were sunny with few clouds and there were very few rain events during the entire study period. Relative humidity (RH) was typically 40–80%. Only about 3% of used data had RH above 85%.

2.2. Experimental setup

Five gas analyzers were evaluated as part of this study (Fig. 1, Table 1). The two open-path sensors were the LI-7500 A and the IRGASON. The two enclosed-path analyzers were the LI-7200 and EC155 (though the system is referred to as CPEC200); they both had inlet tubes of comparable length (˜60 cm). The CPEC200 system used a heated inlet, whereas the LI-7200 did not. The closed-path sensor was a Picarro 2311-f gas analyzer with an 8 m inlet tube. All instruments were mounted on the tripod except the Picarro

analyzer, which was located in a nearby, climate controlled shed along with a data acquisition system. In addition to the gas analyzers, three sonic anemometers were deployed. Multiple sonic anemometers were required to avoid overcrowding a single sonic anemometer as well as minimizing spatial separation between the gas analyzers and sonic anemometers. Additionally, two of the gas analyzers were designed to be integrated with specific sonic anemometers and deploying them independently would compromise their intended use. The CSAT-3 A sonic anemometer (referred to as CSAT) was paired with the EC155 gas analyzer; the combined unit is referred to as the CPEC200. The IRGASON is an integrated system that combines the open-path Campbell Scientific IRGA and a Campbell Scientific CSAT3 sonic anemometer in a single unit. Lastly, a Gill R3-50 sonic anemometer (Gill-Solent, Lymington, UK) was also deployed (referred to as Gill). Details about all instruments and instrument pairing can be found in Table 1.

The CPEC200 has an optional valve module that can be used to perform regular, automated calibration checks. For much of the study period, the valve module was used daily at midnight to deliver zero (ultra-pure nitrogen containing no CO_2 or H_2O) and CO_2 span calibration gases. During this period (˜15 min), ambient measurements were not taken, resulting in loss of flux observations during the first half hour of the day in exchange for calibration data. The calibration procedure involved three 5 min sequences where CO_2 span gas, zero gas, and CO_2 span gas (replicate) were measured. When analyzing calibration data, we identified stable periods during the zero and span calibration procedure and took the mean of the final 100 s. This information was used to test the temperature dependence of the instrument, not to make adjustments. All gas analyzers were factory calibrated before deployment. A post-deployment calibration check was performed but this occurred many months after the data subset presented here. The experimental aim was to deploy and use instruments in a manner comparable to those practiced in the user community.

The relative spatial position of the instruments on the tripod was rearranged halfway through the study period, on July 3, 2015. We refer to the two halves as experiment 1 (exp1) and experiment 2 (exp2). During exp1 (April 7 - July 3), the analyzers without pre-paired anemometers (LI-7200, LI-7500 A, Picarro) were paired with the Gill anemometer, because it was centrally located on the tower (Fig. 1). During exp2 (July 3 - October 6), the CSAT anemometer was centrally located and used as the anemometer for flux calculations for the same three gas analyzers (Fig. 1). The instrument positions were changed to minimize sensor separation and investigate the effect of the anemometers on the gas analyzer fluxes. Sensor separation was generally 30 cm or less (Table 1). Changing the positioning also allowed us to investigate how the experimental setup influenced the measurements.

Eddy covariance data were collected digitally from all instruments at 10 Hz using custom data acquisition software, HuskerFlux (Billesbach et al., 2004). The software read and synchronized the instrument data streams sent via

serial communications and stored the data on a desktop computer, housed in the climate-controlled shed. The data acquisition frequency (10 Hz) was based on the output rate of the slowest instrument, Picarro. All data streams were collected and synchronized using Huskerflux on one computer. The data acquisition system experienced occasional failures (hardware and power), leading to periods with no data. Outages accounted for 14% of the data during experiment 1 and 11% of the data during experiment 2. Ancillary slowresponse (1 Hz) air temperature and radiation data were also collected on a separate nearby tripod. These temperature data were used for EddyPro processing instead of the sonic temperature, except when high-frequency temperature measurements were required.

2.3. Data processing (Quality assurance, filtering, EC processing)

2.3.1. Eddy covariance data processing

An open source eddy covariance software package, EddyPro (version 5.2.1), was used to process the data. Unless otherwise specified, default software settings were used (e.g., block averaging, despiking thresholds, 2-D coordinate rotation, etc.). No angle of attack corrections (Nakai and Shimoyama, 2012; Nakai et al., 2006) were applied to the Gill sonic anemometer since it does not apply to the R3-50 (Billesbach et al., 2019). Temporal lags between the sonic anemometer and the gas analyzer, whether due to digital signal processing delays or physical (separation of sensors or residence time in inlet, were calculated for each averaging period using the covariance maximization procedure. Multiple processing iterations were used to obtain results for the different gas analyzer and sonic anemometer pairings as well as for different spectral correction methods. EddyPro produced 30-minute processed results (full output file) as well as full and binned spectral and cospectral files.

2.3.2. Data filtering

Several measures were taken to quality-control the dataset. The most restrictive filtering was associated with wind direction selection. To avoid turbulence interference from the tripod structure and the nearby shed on the EC measurements, we only considered flux data corresponding to wind directions of 180° ± 60°. This restriction was also necessary to sample the alfalfa because the tower was at the edge of the field. Although the dominant wind direction at the site was from the south (180°), other wind directions occurred 24% of the time during exp1 and 27% of the time during exp2. Therefore, this study is not designed to analyze flow distortion associated with instrumentation form factors and such an investigation is beyond the scope of this manuscript.

Periods with any gas fluxes greater than five standard deviations from the mean were removed as spurious. We also used the data quality flag described by Foken et al. (2004). The open-path sensors were susceptible to obstruction of the path, so we applied minimum signal strength thresholds

for both the IRGASON and the LI-7500A. We determined these thresholds to be 90% of the maximum value for both the LI-7500 A and the IRGASON based on visual inspection of the signal strength time series.

If any of these conditions were met for any instrument, the half-hour period was excluded from the analysis. This strict criterion guaranteed that all comparisons used the same number of data points at the same measurement times. After accounting for all missing and filtered data, about 53% of exp1 and 38% of exp2 half hour fluxes remained. The discrepancy in available data between exp2 and exp1 was largely due to low IRGASON signal strength caused by bird guano for 2–3 weeks.

3. Theory/Calculation

3.1. Spectra and cospectra

A common tool used to analyze the frequency distribution of eddy covariance signals is Fourier spectral analysis (Stull, 1988; Kaimal and Finnigan, 1994; Foken, 2008; Aubinet et al., 2012). Fig. 2 schematically illustrates the main ideas from Sections 3.1 and 3.2.

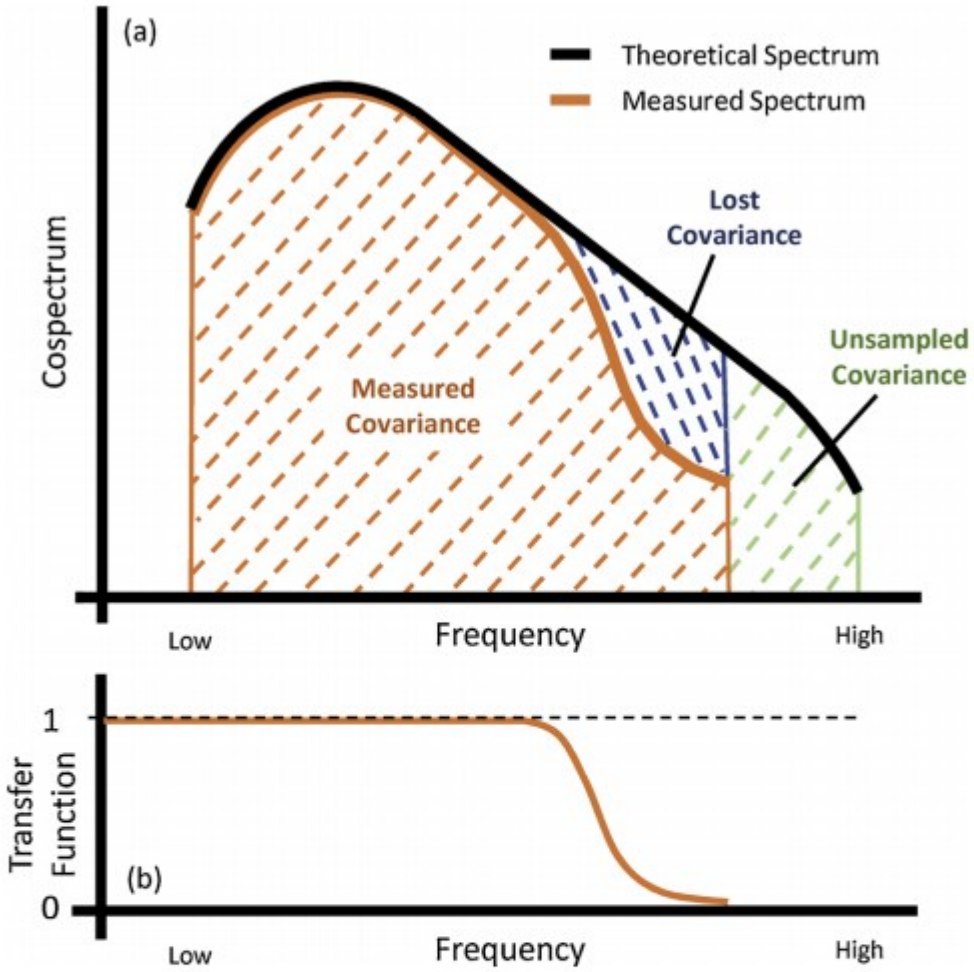

Fig. 2. Schematic figure demonstrating the covariance loss from spectral attenuation. The theoretical cospectrum (black) can be calculated but is often taken to be the w't' cospectrum. Measured gas copsectra (orange) often experience high frequency attenuation. The attenuation typically begins at lower frequencies for closed path gas analyzers than for open path gas analyzers. The integral of the cospectra of the gas and vertical wind speed equals the covariance of those two time series', so more signal loss corresponds to more loss in covariance (and therefore loss of flux). Some covariance is not sampled because it occurs above the Nyquist frequency. The transfer function shown in (b) is the ratio of the true cospectrum to the measured cospectrum and provides an inverse measure for the lost signal at each frequency. The methods for calculating a transfer function vary between spectral correction methods; they can be theoretical or empirical.

First, a Fourier transform is performed on the measured high-frequency, lag corrected time series, $c_s(t)$:

$$F_c(f) = \frac{1}{\sqrt{2}} \int_{-\infty}^{\infty} c_s(t) e^{ift} dt \quad (2)$$

where $F_c(f)$ is the Fourier transformation of the time series of c. From there, the power spectrum is defined as:

$$C_{cc} = F_c(f) \cdot F_c(f)^* \quad (3)$$

where $F_c(f)$ is the Fourier transform of the scalar, c, and $F_c(f)^*$ is the complex conjugate of $F_c(f)$. Similarly, the cospectrum is defined as the real part of:

$$C_{wc} = F_w(f) \cdot F_c(f)^* \quad (4)$$

where $F_w(f)$ is the Fourier transform of the vertical wind speed, w. Besides visually demonstrating signal attenuation, the integrals of the (co)spectra have useful physical significance; by Parseval's Theorem:

$$\int_0^{\infty} C_{cc}(f) df = \sigma_c^2 \quad (5)$$

and

$$\int_0^{\infty} C_{wc}(f) df = \overline{w'c'} \quad (6)$$

where σ_c^2 is the variance of c and $\overline{w'c'}$ is the covariance of w and c, as required to calculate fluxes in Eq. (1). Due to these integral properties, the observed spectra and cospectra are commonly used as a foundation for correction factors when the true frequency spectrum is not adequately measured.

The gas spectra describe the frequency response of the gas analyzer alone, whereas the gas cospectra describe the frequency response of the combined gas analyzer-anemometer EC system. The theory of (co) spectral similarity suggests that the shape of the (co)spectra of scalars are the same (Kaimal et al., 1972). This theory has been shown to hold well in the high-frequency range, which is the focus area of this study (Ruppert et al., 2006).

Flux cospectra are known to experience high-frequency biases for several key reasons, in approximate order from largest to smallest: inlet tube effects for closed and enclosed-path gas analyzers, time delay (if not corrected), flow distortion from instruments and supporting structures, sensor time response, volume and path averaging, spatial separation between the analyzer and the anemometer, and digital sampling artifacts. The kinematic heat flux (the covariance of vertical wind and sonic temperature, $\overline{w'Ts'}$), which is measured only using the sonic anemometer, is commonly assumed to be an unattenuated or "true" cospectrum, though small amounts of

attenuation can occur. The anemometer samples air directly (no inlet tube) and takes colocated measurements of vertical wind and temperature. A visual comparison of the temperature and gas spectra of closed-path analyzers can show a combination of the previously listed frequency-response altering effects.

3.2. Transfer functions and corrections

Insufficient high frequency response of EC systems often needs to be corrected to avoid bias in measurements (Massman and Clement, 2005). Early corrections were analytically derived using a low pass filter description of the attenuation (Moncrieff et al., 1997; Massman, 2000, 2001). Empirical corrections use the calculated spectra or cospectra to calculate a correction factor. In most spectral corrections, a transfer function, TF, is defined to characterize the frequency response of the system in the inertial subrange and subsequently to correct the fluxes (Ibrom et al., 2007a; Fratini et al., 2012). The correction factor, CF, is defined as

$$CF = \frac{\int TF \cdot C_{we}\, df}{\int C_{we}\, df} \qquad (6)$$

We later briefly review the Massman (2000) and Fratini et al. (2012) methods to obtain the TF and subsequent spectral correction factor and discuss a more direct approach using only the measured cospectra. Other methods such as wavelet-based approaches (Nordbo and Katul, 2013) are available but were beyond the scope of this work.

3.3. Spectral correction methods

When comparing fluxes we considered both uncorrected and corrected fluxes. Uncorrected refers to fluxes with no spectral corrections applied for tube attenuation, flow distortion, sensor time response, path averaging, sensor separation, or digital sampling. However, time lag compensation and the Webb-Pearman-Leuning (WPL) term for density fluctuations (Webb et al., 1980) were included in the ‘uncorrected’ flux calculation. We did not consider the pressure perturbations in the density correction (Zhang et al., 2011) because the correction is generally regarded as small.

3.3.1. Massman correction

The Massman spectral correction method is an analytical correction based on characteristics of the environment, instrument, and field site (Massman, 2000, 2001). Massman spectral corrections were implemented by selecting the option in the EddyPro software. The method extends the simple, analytical formula for scalar attenuation developed by Horst (1997) which approximates the scalar sensor as a linear, firstorder instrument with a characteristic time constant. The Massman spectral correction method generalizes this approach to account for scalar attenuation due to a broader suite of cases with described time constants (see Table 1, Massman, 2000).

The method relies on idealized cospectral models based on ensemble-averaged observations and cospectral similarity. The benefits of the Massman correction are that it requires minimal computational time and incorporates multiple sources of signal attenuation.

3.3.2. Fratini correction

The Fratini spectral correction method develops TFs using an empirical approach based on in situ observations (Fratini et al., 2012). Fratini spectral corrections, like the Massman corrections, were implemented by selecting the option in the EddyPro software. The method builds on the framework from Ibrom et al. (2007a), which describe a correction using the ratio of measured sonic temperature and gas spectra to calculate transfer functions. The ratio is then fitted to a first order sensor to obtain a transfer function. The Fratini correction incorporates an additional relative humidity dependence of the transfer function for correcting water vapor fluxes (Fratini et al., 2012). The method fails during low flux periods, which are parameterized separately as functions of wind speed and atmospheric stability. The commonly used first order sensor approximation that is required for the Fratini TFs may not be ideal, especially for H_2O corrections (de Ligne et al., 2010).

The Fratini correction requires the calculation of half-hourly spectra, which makes it computationally intensive. It isolates gas analyzer frequency effects because it only uses spectra, not cospectra, which means that it does not incorporate a correction for sensor separation or other sources of attenuation. Fratini et al. (2012) therefore apply an additional correction for sensor separation (Horst and Lenschow, 2009). We did not apply any corrections for sensor separation when using the Fratini correction method since the Horst and Lenschow method gave very high correction factors, especially during stable conditions. For example, 10% of quality controlled data during exp1 had correction factors over 1.54 from sensor separation alone.

3.3.3. Direct correction

The direct spectral correction method refers to the use of the measured cospectra to account for high-frequency attenuation. This physically fundamental correction relies on only measured cospectra, and was proposed in Massman (2000) but deemed too computationally expensive. A similar method has previously been applied by Su et al. (2004). The motivation for applying the direct correction was to provide a basis for comparison for the other methods, but it could also be used as an operational correction method. This method is adapted from previous work, but is not available in EddyPro.

The steps to calculate the direct method correction factor are outlined in Fig. 3. We start with the ratio of the ensemble median gas and temperature cospectra to obtain a TF. For H_2O flux corrections, TFs were calculated for

relative humidity quantiles (TFs for exp1 can be found in Fig. S3). We chose quantiles to maintain ample data points for averaging and an equal number of spectra in each RH class. The benefit of this method is that it uses the cospectra, which are the basis for determining fluxes. The computational costs are high when using several months of half-hour cospectra with thousands of frequencies, and many cospectra are required to obtain an adequate ensemble of halfhour cospectra which are frequently noisy. However, after cospectra were calculated using EddyPro, all calculations were done using MATLAB code on a standard PC, demonstrating computational costs are manageable by current standards. MATLAB and Python versions of the method are publicly available (see Appendix A). The direct method, like the Fratini method, can lead to unrealistically large correction factors during low flux periods, but since this occurs during periods of very small fluxes, the impacts were limited. We did not see resulting outliers in the data and did not apply any other method for these periods.

The direct method was also found to work for aliased cospectra since the integral of the curves remained the same. However, application of this method is not ideal due to the redistribution of cospectral power. The only alteration of the method for these cospectra is the frequency at which the transfer function is set to 1 is moved from 1 Hz to 0.1 Hz since the aliasing causes energy at higher frequencies to be shifted to lower ones.

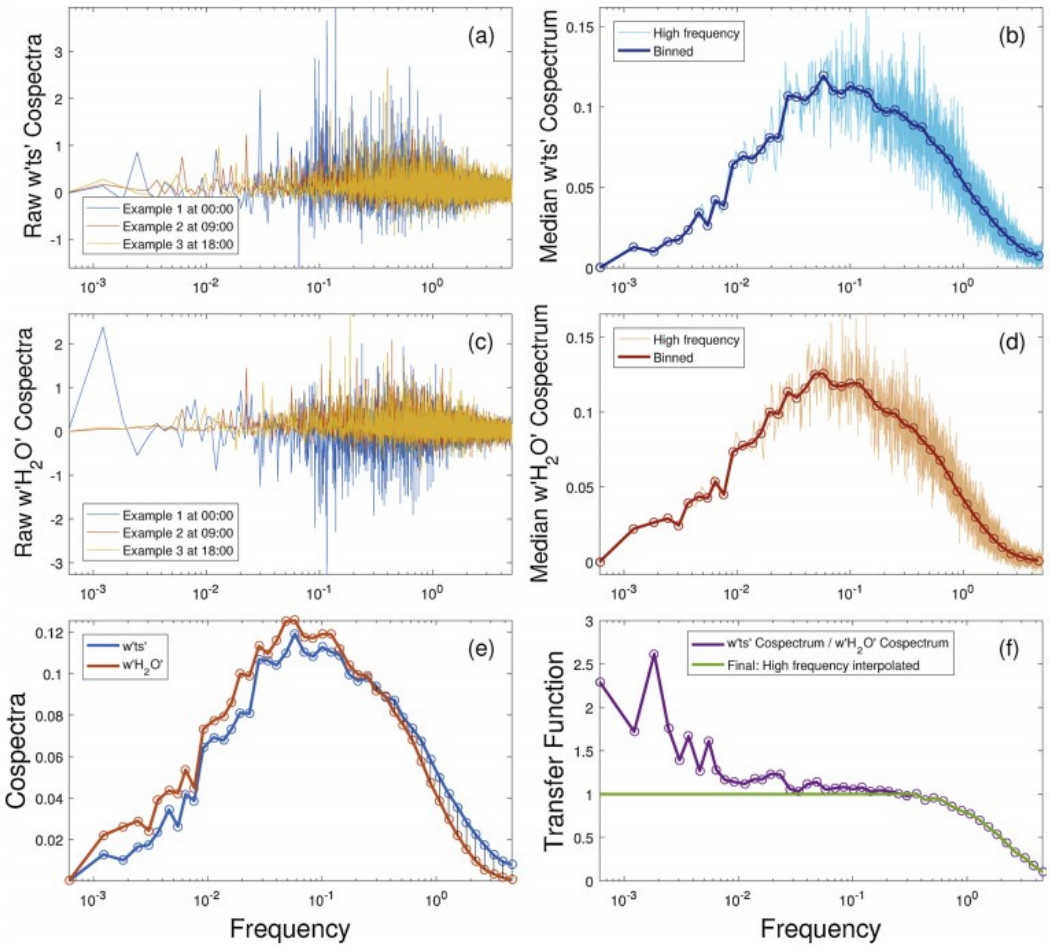

Fig. 3. Calculation progression of direct transfer function. Panels (a) and (c) show examples of high frequency half hour cospectra of sonic temperature and H_2O concentration. The high frequency and binned median of all used half hour cospectra is shown in panels (b) and (c). The binned cospectra from (b) and (c) are plotted together in figure (e). All cospectra are normalized by covariance. The shaded area between them at high frequencies is the result of signal loss. Panel (f) shows the ratio of the cospectra in (e) and the final transfer function (TF), which is set to 1 at frequencies below where the TF becomes greater than 1. The final TF is also linearly interpolated to original, higher frequency resolution. For H_2O fluxes, this process is repeated for each relative humidity quantile to obtain four transfer functions for each system. For sensors with aliased cospectra, the TF is not set to 1 as before, except for frequencies below 10^{-2}.

3.4. Total least squares regressions

Most figures compare two variables that have their own associated errors. Using ordinary linear regression results in an underestimation of regression slopes when the variable on the x-axis has a similar error to the variable on the y-axis (Carroll and Ruppert, 1996). Therefore, unless otherwise noted, all regressions throughout this study are conducted using total least squares (TLS). TLS minimizes the orthogonal residuals of the fit rather than the vertical residuals as with ordinary least squares.

4. Results

4.1. Gas concentrations

All gas analyzers captured similar diurnal trends for both CO_2 and H_2O gas concentrations (Fig. 4). However, concentration offsets in diurnal ensembles were observed, up to 5 ppm for CO_2 and 2 mmol mol^{-1} for H_2O. To examine the diurnal amplitude, the concentration offsets were removed by setting

midnight concentrations equal to the mean of all sensors at that time (Fig. 4c,d). The CPEC200 and IRGASON exhibited higher daytime CO_2 concentrations compared to the other sensors; their diurnal amplitude was about 4 ppm smaller than for the Picarro and LI-7500 A, and 2–3 ppm smaller than for the LI-7200. To evaluate if environmental factors could explain the diurnal differences, we regressed various terms against the concentration differences and found the temperature to have some explanatory power. To further isolate any temperature dependence of the concentration measurements, a linear model was developed:

$$\text{sensor2} = a^{*}\text{sensor1} + (b \cdot T) + c \qquad (7)$$

where *a*, *b*, and *c* are least squares regression coefficients, T is the sonic temperature from the CSAT, and sensor1 and sensor2 are gas concentration measurements from two different gas analyzers. *b* is the temperature coefficient, which gives the temperature dependence of sensor2 compared to sensor1. Other factors that could influence sensor comparisons, such as signal strength, were not included in this analysis.

Each sensor's measurements were modeled against the other sensors using a slope, offset, and temperature term. Applying the linear model, even without the temperature term, decreased the difference in the diurnal CO_2 concentration ensemble between the CPEC200 and the other analyzers (Fig. 4f,h). The IRGASON CO_2 concentration offset remained relatively unchanged, both with and without the inclusion of the temperature term (Fig. 4f,h).

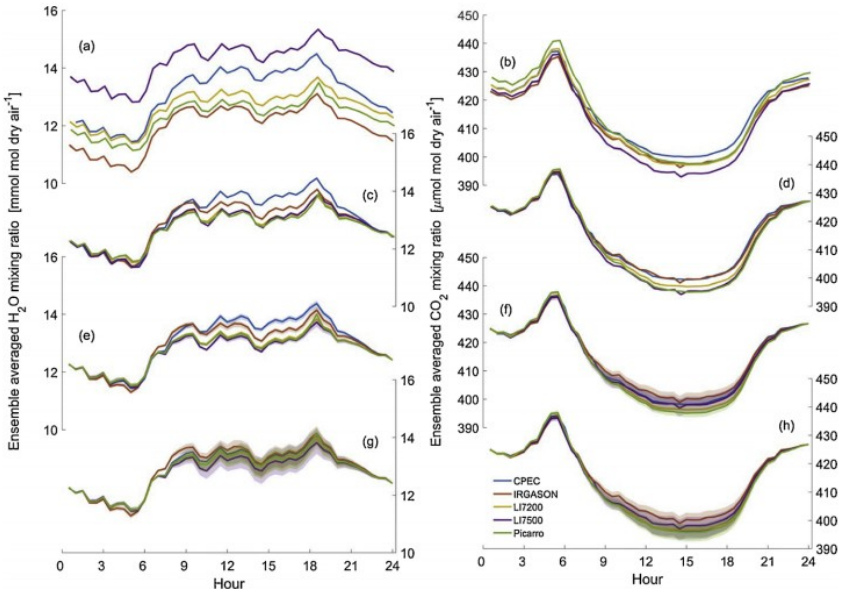

Fig. 4. Diurnal ensemble average of gas concentrations for five gas analyzers during the entire study period. Panels (a) and (b) show ensemble of half hour averages. Panels (c) and (d) are the same as (a) and (b), but with the midnight measurement for each analyzer set to the mean of all five. Panels (e), (f), (g), and (h) are the results of the linear model application, where (e) and (f) exclude the temperature term, and (g) and (h) include the temperature term. Shading represents the minimum and maximum of each linear model result and the line is the mean.

When comparing offset-removed diurnal ensemble average H_2O concentrations, a similar elevated concentration measurement was observed for the CPEC200 and IRGASON as was noted for CO_2 concentrations (Fig. 4c). However, the linear model without a temperature term did not improve the

comparison (Fig. 4d). The CPEC200 only aligned well with the other sensors upon the inclusion of temperature as an explanatory factor (Fig. 4g). All linear model temperature terms can be found in the supplementary materials (Fig. S1).

Analysis of the CPEC200 automatic calibration measurements also demonstrated a temperature sensitivity. Using the change in the slope between daily zero and span measurements as a function of temperature resulted in 0.046%/K and 0.048%/K for the 455.57 ppm CO_2 and 381.7 ppm CO_2 span gases, respectively. No span measurement was available for H_2O, so only an ordinary linear least squares regression between the zero measurement and temperature was possible; this showed a sensitivity of 0.02 mmol/(mol K). This analysis was made possible by the availability of the CPEC200 integrated calibration system and the results are well within the instrument specifications of 0.1%/K for CO_2 and ± 0.05 mmol/(mol K) for H_2O. The calibration information could also be used to correct for temperature dependencies or drifts associated with pressure and signal loss due to contamination of the optical windows.

4.2. Anemometers and data quality

We compared sonic anemometer measurements during exp1 and exp2 to look for systematic differences between sensors and to assess the influence of relative placement on the tower. Rotated crosswind speed variances ($\overline{v'v'}$) and vertical wind speed variances ($\overline{w'w'}$) measured by the Gill and the CPEC compared well during both experiments (Fig. 5c,d,e,f). The IRGASON measured 15% higher *v* variance for both experiments (Fig. 5c,d), which is consistent with previous wind tunnel and field experiments (Horst et al., 2016). The IRGASON measured about 5% lower *w* variances for both experiments (Fig. 5e,f), whereas Horst et al. (2016) found differences under 0.5%. Our dense instrument setup was not ideal for analyzing flow distortions, but the lower IRGASON *w* variance was consistent for both experimental setups. Wind speed and $\overline{u'u'}$ comparisons differed slightly between exp1 and exp2 (Fig. 5a,b,g,h), which suggested that the dense placement of the instruments had some effect on the sonic anemometer measurements. The sensible heat flux from the CPEC and IRGASON were within 2% for both experiments, and the Gill was no more than 9% higher in both experiments (Fig. 5i,j). The momentum flux, as a derived quantity, shows more differences between anemometers than the other comparisons, which has previously been observed (Mauder and Zeeman, 2018). The bias in the IRASON v variance will also affect this result (Horst et al., 2016). However, we do not suspect that these effects have a large impact on vertical fluxes after filtering for wind direction based on the similar regressions for $\overline{w'w'}$ in Fig. 5c and h.

Our data quality filters were chosen to minimize the influence of the shed and tower on the results. The effect if wind direction and signal strength filtering can be found in the Supplementary Fig. S2.

4.3. Spectra and cospectra

The gas concentration spectra demonstrated high-frequency attenuation for different sensors. For CO_2, most of the gas analyzers had very similar spectral signatures but substantial attenuation was visible for the Picarro (Fig. 6a,c). H_2O signal attenuation was clearly visible for the Picarro as well as the two enclosed-path instruments. As expected, open-path sensors showed the least high-frequency attenuation. Both enclosed-path sensors exhibited similar magnitudes and the closed-path Picarro had the most loss of high-frequency signal (Fig. 6). Though it is not possible to identify the exact causes for the attenuated spectral shapes, the likely sources are the tube length, mixing of the flow within the inlet system (filter, joints, etc.), and the time response of the gas analyzers themselves.

The cospectra of CO_2/H_2O and the vertical wind component captured the high-frequency attenuation from the gas analyzers as observed in the spectra (Fig. 6) as well as signal loss from additional factors such as the separation of the eddy covariance sensors. Sensor separation is one possible explanation for the difference in attenuation of the two open-path systems; the IRGASON has had collocated sensors, whereas the LI-7500 A had some horizontal sensor separation.

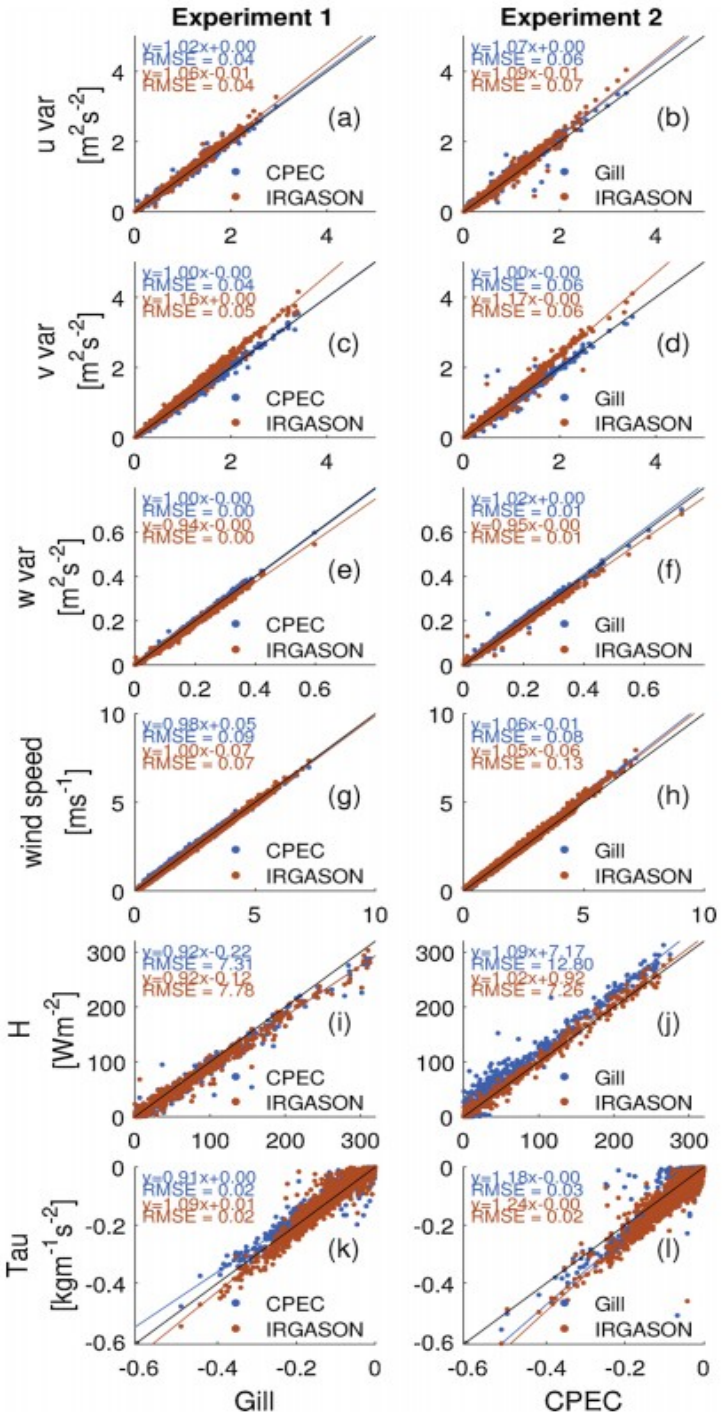

Fig. 5. Sonic anemometer comparison. Wind variances of all three sonic anemometers, with the center anemometer on the x-axis. (a)–(f) show u, v, w variances (g)–(h) show wind speed (i)–(j) show sensible heat flux, and (k)–(l) show momentum flux. The left column shows exp1 and the right column shows exp2.

The LI-7200 and the LI-7500 A had aliased cospectra during exp2, when paired with the CSAT anemometer (Fig. 6g,h) (Moore, 1986; Burba, 2013). Aliasing generally refers to high frequency fluctuations that are translated to

lower frequencies in a sepectrum or cospectrum. This shift can occur through sampling at insufficiently high frequencies or through step changes in the data or filters that are challenging to represent through sines and cosines and therefore cause fluctuations. Sampling frequency and bandwidth settings were consistent among all gas analyzers during both experiments. The aliasing was observed for both experiments with this pairing, but is only seen during exp2 because the shown pairing for exp1 uses the Gill anemometer due to sensor separation considerations. There is no evidence that the LI-7200 or the LI-7500 A were the source of the aliasing. Fratini et al. (2018) demonstrated that small differences in timing (both random and synthetic) of paired instruments can cause distorted cospectra and errors in fluxes. We were unable to find any evidence of timing errors within our data acquisition system, but an unknown timing difference may have contributed to the observed aliasing.

Fig. 7 shows the cospectra of vertical wind and sonic temperature for both experiments for all of the sonic anemometers used during both experiments. All anemometers have similar sonic temperature cospectra. Small differences in the high frequency cospectra (> 2 Hz) were observed between the Gill and CSAT/IRGASON during exp1. High frequency signal loss could be attributed to path averaging, volume averaging, or signal processing but further exploration is beyond the scope of this paper. These differences are small compared to differences in CO_2 and H_2O cospectra (Fig. 6). Therefore, these differences do not introduce large errors the direct method.

4.4. Cross-sensor flux comparison

The differences in turbulent fluxes between sensors varied widely across the different correction methods, especially for H_2O fluxes. Figs. 8 and 9 show all comparisons for exp1; the equivalent figures for exp2 can be found in the supplementary material (Figs. S4, S5). Uncorrected H_2O fluxes were found to match reasonably well only when similar sensor types were compared. Excluding the Picarro analyzer, uncorrected CO2 fluxes matched well (< 4% for exp1, < 6% for exp2) even across different sensor types. Including the Picarro analyzer, uncorrected fluxes differed by as much as 15% for CO_2 (Figure S4, exp2 IRGASON vs Picarro) and 44% for water vapor (Fig. S5, exp2 IRGASON vs. Picarro).

CO_2 fluxes calculated from both experiments using the Massman, Fratini, and direct methods averaged differences of 3%, 3%, and 2% respectively (Figs. 8,S4,9). H_2O flux (Figs. 9,S5,10) differences using the Massman, Fratini, and direct methods averaged 13%, 4%, and 8%. The Massman method resulted in differences under 7% when excluding Picarro and exp1 LI-7500 A fluxes. During exp1, the LI-7500 A H_2O fluxes were 10–28% higher than for other sensors but during exp2, we did not observe this difference. A likely contributor is that the LI-7500 A had 14% and 4% higher H_2O variances compared to the IRGASON during exp1 and exp2, respectively. The LI-7500 A was repaired during the beginning of exp2 due to a chopper motor failure,

and was re-calibrated. Data collected with the broken motor was excluded from the study. Sensor drift or poor calibration was the likely explanation for the elevated H_2O variances and fluxes of the LI-7500 A during exp1. Using the Massman method, fluxes originating from the Picarro setup consistently underreported fluxes in comparison to the other instrument setups by around 15% and 25% for exp1 and exp2, respectively. In contrast, the Fratini and direct methods normally performed at least 10% better, but also still underestimated fluxes.

Fig. 10 summarizes the regression slopes shown in Figs. 8,9,S4,S5. The direct performs best for CO_2 fluxes, although all methods performed well. The Fratini method performs best for H_2O fluxes, followed by the direct method.

4.5. Spectral correction magnitudes

In addition to comparing EC systems with different spectral correction methods, we also examined the relative differences between correction methods within a given EC system. The correction factor (CF) magnitude is relevant because even if two different spectral correction methods effectively align fluxes from different sensor types, they may still result in different flux values. For example, if average uncorrected fluxes from one sensor were half of another, the average CFs 2 and 1 would align the fluxes, but as would average CFs of 3 and 1.5, but the resultant flux magnitude would be very different in each case. Fig. 11 summarizes the CFs for each system and correction method during both experiments. The percent difference between each method for an individual EC system describes the change in the magnitude of the final fluxes. Most CO_2 CFs ranged from 1 to 1.2 and most H_2O CFs ranged from 1 to 2 (Fig. 11). No correction method consistently yielded larger or smaller corrections for CO_2, but H_2O CFs from the Massman method were generally smaller than from Fratini or direct methods.

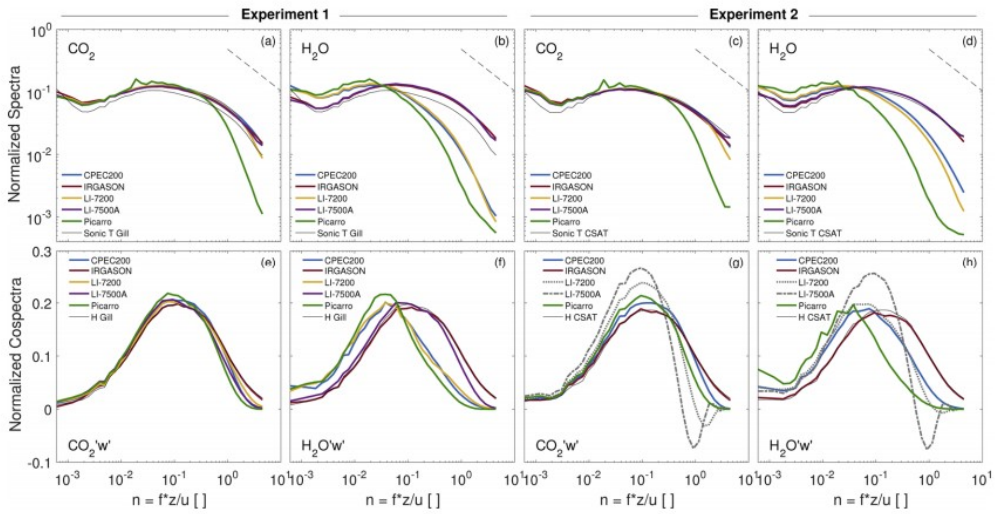

Fig. 6. Ensemble average, normalized gas (co)spectra from all data during exp1 and exp2 with the ensemble average sonic temperature spectrum for reference are shown in (a)-(d). Normalized frequency, n, is scaled by the observation height, z, and horizontal wind speed, u. Deviation of the gas spectra from the sonic temperature spectrum at high frequencies is attributed to signal attenuation from the inlet tube. A -⅔ slope is shown for reference (dashed line, (a)-(d)). Spectra isolate the attenuation due to only the gas analyzer. Similarly, ensemble gas cospectra are shown in (e)-(h) on a linear scale. Aliasing of the LI-7200 and LI-7500 A cospectra when paired with the CSAT anemometer during exp2 can be seen in (g) and (h). Cospectral attenuation is primarily a combination of tube effects and sensor separation.

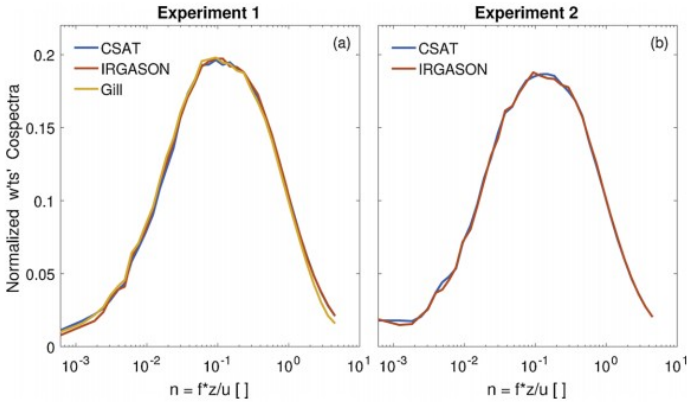

Fig. 7. Normalized cospectra of vertical wind and sonic temperature from the used sonic anemometers during experiment 1 (a) and experiment 2 (b). Data from Gill R3-50 anemometer were not used in experiment 2.

The median of the CO_2 correction factors for each system usually did not differ by more than about 5% (Fig. 11). The largest difference between methods occurred for the IRGASON; the Fratini method increased CO_2 fluxes by 2–15%, whereas the direct method, with very little variation, added less than 1%. The range of all Fratini CFs remained roughly constant for both open-path systems. Since open-path sensors do not have tube effects, and the Fratini method only uses measured spectra, the similarity between CO_2 and H_2O CFs was expected. The minimal sensor separation of the IRGASON would theoretically decrease the required spectral correction, which can be seen in the small magnitude of the direct method corrections. Though not explored in this study, any flow distortions from the IRGASON form factor may not be captured by the direct spectral correction method if the gas and sonic temperature cospectra experienced the same distortions. The Massman H_2O corrections for closed and enclosed-path sensors were lower

than the Fratini and direct methods, which suggested that it underestimated H_2O tube effects. The clearest example of this was the Picarro analyzer, for which the median Massman correction was about 10% for both experiments, and the median Fratini and direct method corrections were about 36% for exp1 and 45–55% for exp2.

Correction method differences of 5–10% were common even for the sensors that appeared to have relatively consistent CFs on Fig. 11, which emphasizes the importance of the chosen method. Fig. 12 also emphasizes the differences between correction methods and sensors by evaluating the change in cumulative fluxes for CO_2 and H_2O. Cumulative fluxes, despite the gaps for missing or quality controlled data, illustrate how CF differences could impact longer-term (e.g. yearly) sums when considering net ecosystem exchanges.

5. Discussion

5.1. Sensor types

All EC systems tested in this study can be used to effectively measure ecosystem CO_2 and H_2O concentrations and fluxes, given that users take the relevant precautions such as applying spectral corrections when necessary and excluding data from flow-distorted wind directions. The gas concentration power spectra showed a clear distinction between sensor types. The difference between systems with an inlet tube and open-path systems was more pronounced than the difference between closed and enclosed-path sensors. Sensor type differences remained visible in the cospectra, but were confounded with additional attenuation sources beyond tube attenuation (e.g., sensor time response, path averaging, sensor separation, sensor response mismatch, digital sampling, etc.).

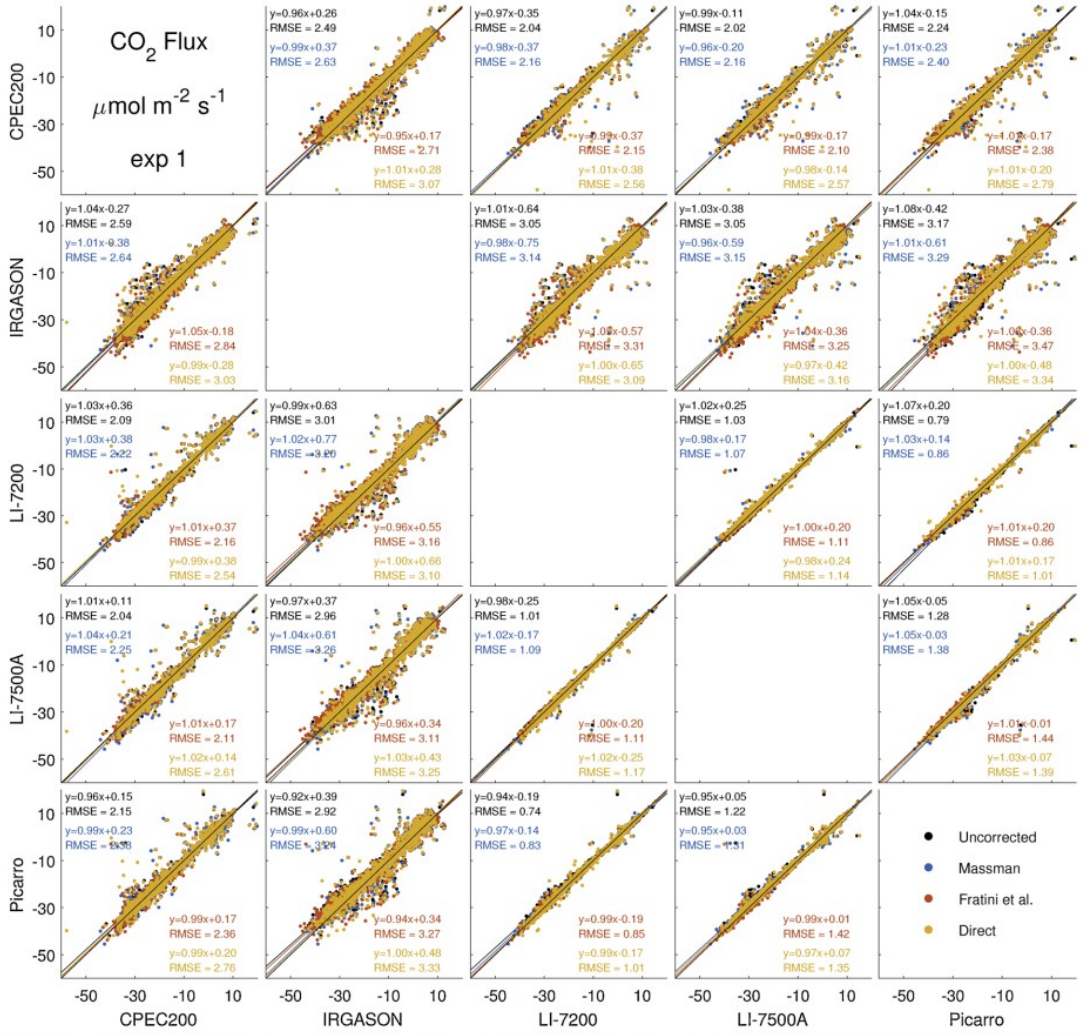

Fig. 8. Scatter plot matrix of CO_2 fluxes [μmol m-2 s^{-1}] during exp1 for uncorrected fluxes and fluxes corrected using the (Massman, 2001; Fratini et al., 2012), and direct methods. Linear regression results and root mean square error (RMSE) are shown. Black 1-1 line included for reference.

5.2. Use of spectral corrections

The cospectra revealed evidence of high-frequency losses likely due to tube effects and contributions from other sources such as sensor time response, path averaging, sensor separation, sensor response mismatch, digital sampling, etc. The IRGASON, which had neither an inlet tube nor sensor separation, had gas cospectra that matched the sonic temperature cospectrum very well (Fig. 6). The results using the direct spectral correction method suggested that no large errors would be introduced by excluding spectral correction from data processing for the IRGASON. The colocation of the sonic anemometer transducers and the gas analyzer has the potential to cause flow distortion (Horst et al., 2016). Such distortions may be missed by the direct spectral correction method if there are equal effects of distortion on the cospectra of vertical wind and gas concentration and the cospectra of vertical wind and sonic temperature. However, we saw little evidence of such distortions affecting vertical fluxes or cospectra (Fig. 7), especially given the

limited wind direction regime that we analyzed for this study. During both experiments, the vertical wind variance measured by the IRGASON was about 5% lower than the variance measured by the other sonic anemometers (Fig. 5), which could introduce instrument differences that are not captured by the spectral correction models used in this study. Horst et al. (2016) only found similarly low vertical wind variances when transducer shadowing corrections were applied to the anemometer used for comparison, which was not done in this study. The variance of the crosswind, v, measured by the IRGASON was 15% higher than those of the other anemometers (Fig. 5), which does not impact vertical fluxes directly, but could also introduce errors in momentum fluxes and in footprint models used for analysis of fluxes.

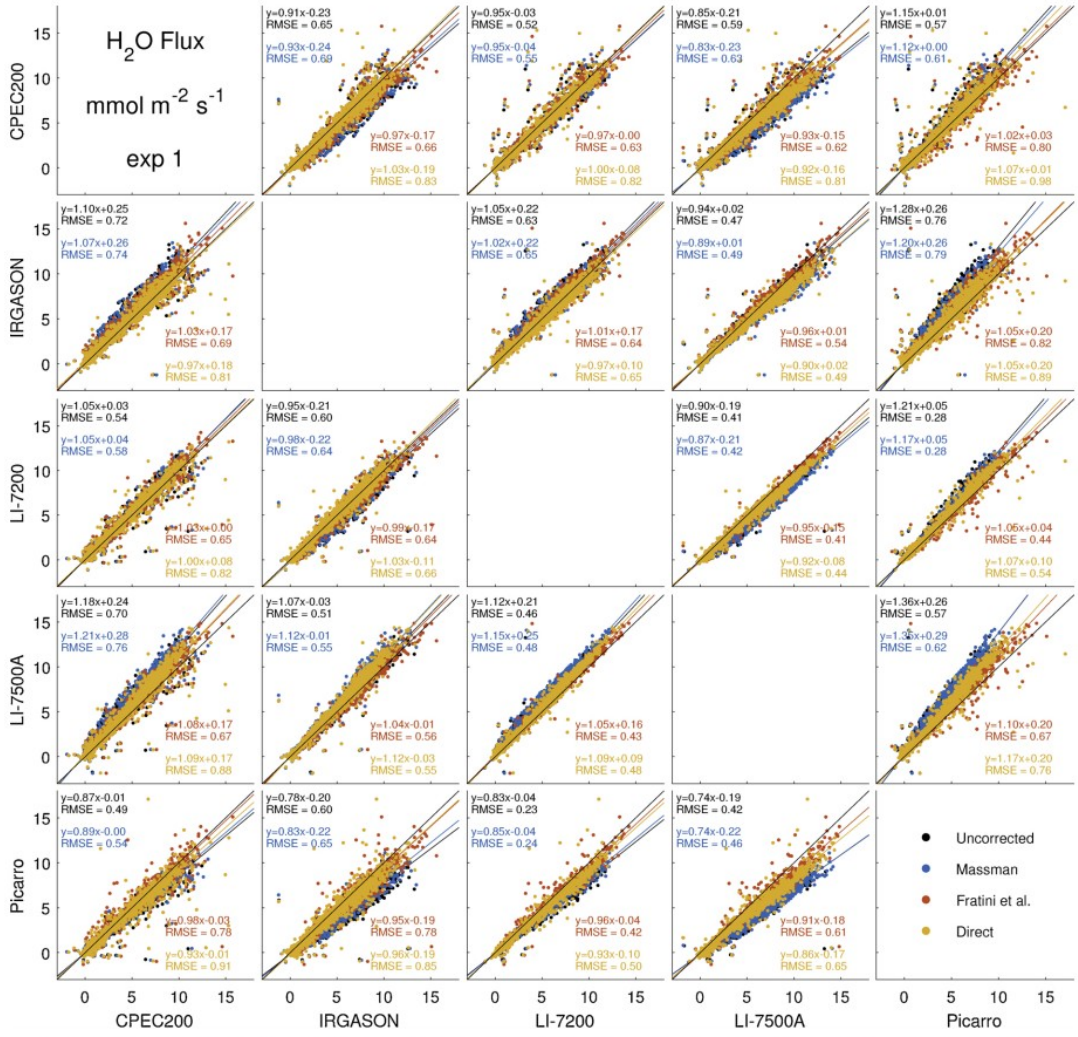

Fig. 9. Scatter plot matrix of CO_2 fluxes [μmol m 2 s^{-1}] during exp2 for uncorrected fluxes and fluxes corrected using the (Massman, 2001; Fratini et al., 2012), and direct methods. Linear regression results and root mean square error (RMSE) are shown. Black 1-1 line included for reference.

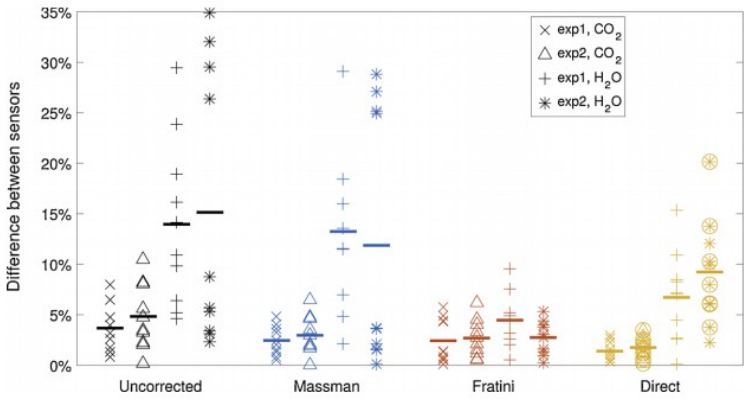

Fig. 10. Summary of percent difference between all sensors for different spectral correction methods for CO_2 and H_2O fluxes for exp1 and exp2. Horizontal lines denote the average for each category. Circles indicate the use of aliased cospectra.

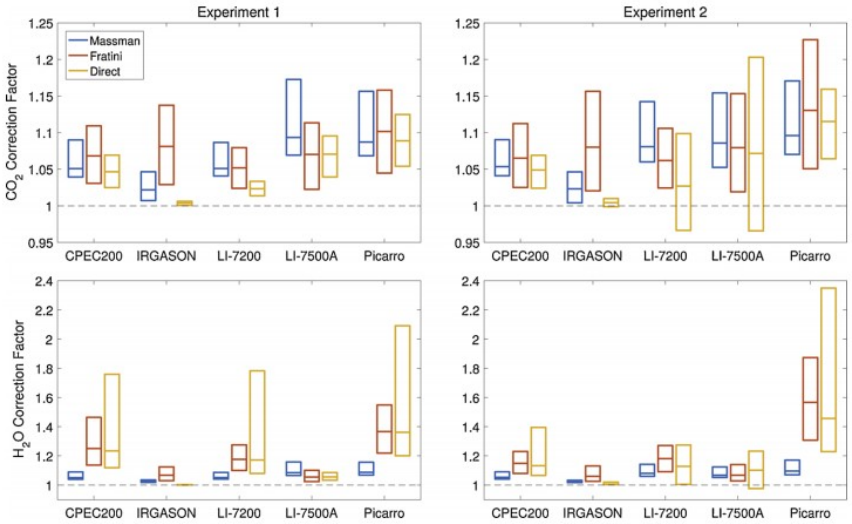

Fig. 11. Box plot of CO_2 (top) and H_2O (bottom) spectral correction factors for each eddy covariance system during experiment 1 (left) and experiment 2 (right), for three correction methods (colored). Each box shows the 25th, 50th, and 75th percentiles of correction factors for the filtered fluxes. The dashed horizontal line indicates a correction factor of 1 (no spectral correction).

CO_2 and H_2O fluxes often agreed between the different eddy covariance systems within about 7% and 20%, respectively, after applying spectral corrections. Assuming the methodological uncertainty of EC is 10–20% (Schmidt et al., 2012), no sensors were substantially different from the others with the exception of underestimated H_2O fluxes from the long-inlet Picarro. However, the effect of the chosen spectral correction was large. Sensors with an inlet tube clearly require spectral corrections for H_2O fluxes. The comparability of sensors varied with the chosen correction method and the magnitude of each correction can differ substantially (Fig. 11). The applied spectral corrections (both magnitude and method used) should therefore be reported, especially when investigators compare EC data from different sites and different sensor types. Lastly, the Fratini et al. (2012) method is not well suited for open-path sensors because it only considers scalar attenuation, which is smallest in open-path sensors. The relatively small scalar attenuation makes the cut-off frequency difficult to define for those sensors. The results from direct method for the IRGASON suggest that very minimal spectral corrections are required.

Users of EC data from some flux databases currently do not have the option to evaluate the magnitude or accuracy of spectral corrections. However, it is important for users to be aware that corrections may have substantial effects on fluxes. Databases, if they do not already do so, should require reporting the name of correction used and preferably also the magnitude of corrections. A framework for the collection of ancillary data (e.g. data processing steps) is currently in development for the AmeriFlux network. The availability of average spectra or cospectra could also improve the ability of both data providers and data users to quickly evaluate whether spectral corrections may be important.

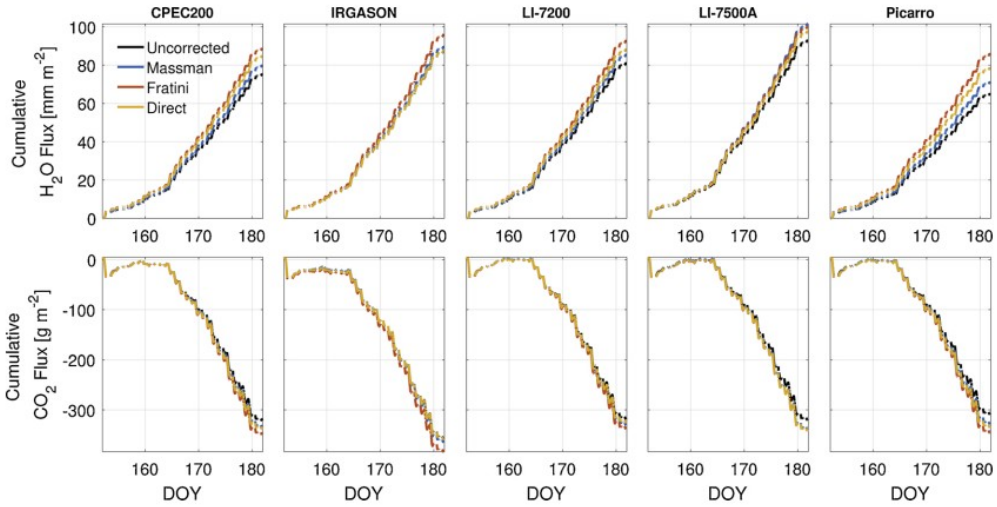

Fig. 12. Cumulative H_2O fluxes for filtered data during June 2015 without gap filling. Each panel shows a different sensor pair (top: H_2O; bottom: CO_2) and each line shows fluxes with no, Massman, Fratini, or direct spectral corrections. Cumulative fluxes give a visual representation of potential differences that ensue from different sensors and corrections.

Table 2
Table to guide decision of EC systems.

	Open path	Enclosed path	Closed path
Relative high frequency attenuation	Low	Medium/High	High
Correction for air density fluctuations	Potentially large	Small	Small
Relative precipitation performance	Poor	Good	Good
Sensitivity to environmental conditions (hydrometeors, guano)	High	Low	Low
Surface heating correction consideration	Yes	No	No
Automated calibration possible?	No	Yes	Yes
Energy usage	Low	Medium	High
Enclosure required	No	No	Yes
Use of filters	No	Possible	Possible

5.3. Uncertainty in EC measurements

EC uncertainties arise from random sampling errors (e.g. sampling of turbulence, random instrument error) and from systematic errors (e.g. instrument design, imperfect corrections) (Aubinet et al., 2012, Chapter 7; Schmidt et al., 2012). Random error estimates as described by Finkelstein and Sims (2001a, b) were calculated by EddyPro and were generally 4–15% of flux measurements. These errors often correlated between different EC systems and therefore cannot be used as an acceptable margin of error between systems, but rather as an estimate of inherent methodological

errors. The spectral correction method differences observed in our study (Fig. 10) were often of a similar magnitude. However, the correction method errors are systematic and would result in a consistent underestimation or overestimation rather than a random error. A rigorous error analysis could be conducted for analytic spectral correction methods like the Massman method, but not for empirical ones like the Fratini or direct methods. Random errors cannot be easily reduced by a user, but the conscious use of spectral corrections can help reduce systematic errors.

5.4. Limitations

This study was set up to compare several key metrics of eddy covariance performance (e.g., concentrations, spectra, cospectra and CO_2 and H_2O fluxes) from a set of the common gas analyzer and sonic anemometer models available at the time. The study was conducted with a small tower over short vegetation, and for a segment of the wind directions coming straight into an anemometer-analyzer pair. It was therefore not possible to conduct a detailed analysis of other potential flux losses such as flow distortion, data collection methods, and time clocking schemes. The importance of the spectroscopic correction was not addressed here, but has been addressed by Helbig et al. (2016), in part using data also used in this study.

The study was conducted with a small tower over short vegetation. The magnitude of spectral corrections would likely decrease at sites with taller towers located over taller canopies (e.g. forest sites), because the peak of the turbulence spectrum shifts towards lower frequency with increasing displacement height (Kaimal et al., 1972). The importance of the spectral correction can be visualized by comparing the normalized gas (co)spectra to the sonic temperature (co)spectrum. Since average spectra and cospecta are available from most eddy covariance processing software packages, visualization is possible with relatively little inconvenience for spot checks.

The Davis, CA field site is inherently relatively dry compared to other environments worldwide. High RH usually only occurs at night, when fluxes are small. This means that for other sites, the RH dependence of fluxes could result in larger difference (for more humid sites) or smaller differences (for less humid sites) between sensor types. Findings could be broadened by using the AmeriFlux Tech Team site visit data, where multiple gas analyzers are regularly deployed at different locations across the AmeriFlux network.

5.5. Choosing a sensor

When choosing an EC system for a field site, several factors should be considered. Table 2 provides a summary of sensor type pros and cons. Open-path sensors clearly minimize spectral attenuation and therefore also require smaller spectral correction factors than sensors with an inlet tube, especially for water vapor fluxes. High-frequency losses of H_2O signal from inlet tubes increase substantially with relative humidity, especially for RH above ˜60%,

which means that humid sites are more strongly affected. However, open-path sensors can experience data outages in non-ideal conditions like precipitation, fog, dew formation, dust, spiders, birds, etc. They also lose signal strength over time due to the collection of atmospheric aerosol and therefore need to be cleaned regularly. Inlets and filters for closed and enclosed systems can also get dirty or degrade over time and need to be replaced (Leuning and Judd, 1996; Mammarella et al., 2009). EC practitioners need to weigh the site-specific benefits of high-frequency response against potential data loss from environmental exposure and subsequent gapfilling measures. The open-path systems have also been shown to overestimate small CO_2 fluxes in cold environments, which has been attributed to surface-heating (Burba et al., 2008), but overestimation has also been shown to persist in sensors with little surface heating (Wang et al., 2017). The closed-path system used in this study did not provide benefits for EC over the enclosed-path systems and experienced the most spectral attenuation and should therefore only be used if the sensor cannot be placed on the tower directly for logistical reasons. However, the Picarro instrument used in this study could also simultaneously measure methane (and potentially other trace gases such as COS and N_2O), which is a benefit that the other instruments could not provide.

Instruments are constantly being developed and some sensors tested here have already been improved or superseded by newer versions. LICOR has released the LI-7500RS and LI-7200RS (2015), which claims to improve sensor performance in the presence of dirt and rain, and LI7500DS (2017), which claims to keep improve the performance over the RS models but with reduced power consumption and price. Campbell has released a new vortex inlet tube for the CPEC200, which claims decrease maintenance intervals and increase frequency response (Ma et al., 2017); it is also included in the newer CPEC300 (2018) system. When changes are implemented, users should remain cognizant of possible impacts to fluxes, especially when comparing to data collected with different instrumentation.

6. Conclusion

We evaluated five gas analyzers and three sonic anemometer models commonly used in eddy covariance flux measurements. Although this study is limited by the use of a single field deployment from limited wind directions, our results highlight signal attenuation associated with different sensor types, as well as the importance of spectral corrections in eddy covariance measurements. We applied three different spectral correction methods (Massman, Fratini, and direct) to address both of these issues. These correction methods had varying degrees of success and the empirical approaches (Fratini and direct) proved to be more successful, in particular to water vapor flux measurements. Despite these differences, after application of spectral corrections, fluxes were comparable between setups (typically within 5% CO_2 and 12% for H_2O), despite large differences in inlet geometry. Data providers and users of eddy covariance data should be aware of the

potentially large differences in fluxes due to sensors types and the effects of correction methods. Furthermore, data users should be aware of such differences, in particular in network-wide synthesis studies. These results emphasize the need for regional flux networks to accurately report metadata that includes data processing methods and sensor characteristics.

Acknowledgements

The work was supported by the Office of Biological and Environmental Research in the U.S. DOE Office of Science as part of Terrestrial Ecosystem Science Program under the Contract DEAC0205CH11231 to the Lawrence Berkeley National Laboratory. All gas systems used in this work were provided on loan from the manufacturers. Thanks to Sigrid Dengel for assistance with text edits.

Appendix A. Supplementary data

Supplementary material related to this article can be found, in the online version, at doi:https://doi.org/10.1016/j.agrformet.2019.02. 010. Direct method MATLAB and Python scripts are publicly available at https://github.com/ppolonik2/AmeriFlux.

References

Aubinet, M., Vesala, T., Papale, D. (Eds.), 2012. Eddy Covariance. Springer, Netherlands, Dordrecht.

Baldocchi, D., Falge, E., Gu, L., et al., 2001. FLUXNET: a new tool to study the temporal and spatial variability of ecosystem-scale carbon dioxide, water vapor, and energy flux densities. Bull. Am. Meteorol. Soc. 82, 2415–2434. https://doi.org/10.1175/ 1520-0477(2001)0822.3.CO;2.

Billesbach, D.P., Fischer, M.L., Torn, M.S., Berry, J.A., 2004. A portable eddy covariance system for the measurement of ecosystem-atmosphere exchange of CO2, water vapor, and energy. J. Atmos. Ocean Technol. 21, 639–650. https://doi.org/10.1175/1520- 0426(2004)0212.0.CO;2.

Billesbach, D.P., Chan, S.W., Cook, D.R., Papale, D., Bracho-Garrillo, R., Verfallie, J., Vargas, R., Biraud, S.C., 2019. Effects of the Gill-Solent WindMaster-Pro “w-boost” firmware bug on eddy covariance fluxes and some simple recovery strategies. Agric. For. Meteorol. 265, 145–151. https://doi.org/10.1016/j.agrformet.2018.11.010.

Burba, G., 2013. Eddy Covariance Method for Scientific, Industrial, Agricultural, and Regulatory Applications: A Field Book on Measuring Ecosystem Gas Exchange and Areal Emission Rates. LI-COR Biosciences, Lincoln, NE.

Burba, G.G., McDermitt, D.K., Grelle, A., et al., 2008. Addressing the influence of instrument surface heat exchange on the measurements of CO2 flux from open-path gas analyzers. Glob. Chang. Biol. 14, 1854–1876. https:// doi.org/10.1111/j.1365-2486. 2008.01606.x.

Burba, G., Schmidt, A., Scott, R.L., et al., 2012. Calculating CO2 and H2O eddy covariance fluxes from an enclosed gas analyzer using an instantaneous mixing ratio. Glob. Change Biol. 18, 385–399. https://doi.org/10.1111/j.1365-2486.2011.02536.x.

Carroll, R.J., Ruppert, D., 1996. The use and misuse of orthogonal regression in linear errors-in-variables models. Am. Stat. 50, 1–6. https://doi.org/10.1080/00031305. 1996.10473533.

Cheng, Y., Sayde, C., Li, Q., et al., 2017. Failure of Taylor's hypothesis in the atmospheric surface layer and its correction for eddy-covariance measurements. Geophys. Res. Lett. 44, 4287–4295. https://doi.org/10.1002/2017GL073499.

Clement, R.J., Burba, G.G., Grelle, A., et al., 2009. Improved trace gas flux estimation through IRGA sampling optimization. Agric. For. Meteorol. 149, 623–638. https:// doi.org/10.1016/j.agrformet.2008.10.008.

Crosson, E.R., 2008. A cavity ring-down analyzer for measuring atmospheric levels of methane, carbon dioxide, and water vapor. Appl. Phys. B: Lasers Opt. 403–408.

de Ligne, A., Heinesch, B., Aubinet, M., 2010. New transfer functions for correcting turbulent water vapour fluxes. Bound.-Layer Meteorol. 137, 205–221. https://doi. org/10.1007/s10546-010-9525-9.

Dyer, A.J., 1981. Flow distortion by supporting structures. Bound.-Layer Meteorol. 20, 243–251. https://doi.org/10.1007/BF00119905.

Finkelstein, P.L., Sims, P.F., 2001a. Sampling error in eddy correlation flux measurements. J. Geophys. Res. 106 (3503).

Finkelstein, P.L., Sims, P.F., 2001b. Sampling error in eddy correlation flux measurements. J. Geophys. Res. Atmos. 106, 3503–3509. https://doi.org/10.1029/ 2000JD900731.

Finnigan, J.J., Clement, R., Malhi, Y., et al., 2003. A re-evaluation of long-term flux measurement techniques part I: averaging and coordinate rotation. Bound.-Layer Meteorol. 107, 1–48. https://doi.org/10.1023/A:1021554900225.

Foken, T., 2008. Micrometeorology. Springer, Berlin Heidelberg, Berlin, Heidelberg.

Foken, T., Goeckede, M., Mauder, M., et al., 2004. Post-field data quality control. Handbook of Micrometeorology: A Guide for Surface Flux Measurement and Analysis. pp. 181–208.

Frank, J.M., Massman, W.J., Ewers, B.E., 2013. Underestimates of sensible heat flux due to vertical velocity measurement errors in non-orthogonal sonic anemometers. Agric. For. Meteorol. 171–172, 72–81. https://doi.org/10.1016/j.agrformet.2012.11.005.

Frank, J.M., Massman, W.J., Swiatek, E., et al., 2016. All sonic anemometers need to correct for transducer and structural shadowing in their velocity measurements. J. Atmos. Ocean Technol. 33, 149–167. https://doi.org/10.1175/JTECH-D-15-0171.1.

Fratini, G., Ibrom, A., Arriga, N., et al., 2012. Relative humidity effects on water vapour fluxes measured with closed-path eddy-covariance systems with short sampling lines. Agric. For. Meteorol. 165, 53–63. https://doi.org/10.1016/j.agrformet.2012.05.018.

Fratini, G., Sabbatini, S., Ediger, K., et al., 2018. Eddy Covariance flux errors due to random and systematic timing errors during data acquisition. Biogeosci. Discuss. 1–21. https://doi.org/10.5194/bg-2018-177.

Grare, L., Lenain, L., Melville, W.K., 2016. The influence of wind direction on Campbell scientific CSAT3 and Gill R3-50 sonic anemometer measurements. J. Atmos. Ocean Technol. 33, 2477–2497. https://doi.org/10.1175/jtech-d-16-0055.1.

Haslwanter, A., Hammerle, A., Wohlfahrt, G., 2009. Open-path vs. closed-path eddy covariance measurements of the net ecosystem carbon dioxide and water vapour exchange: a long-term perspective. Agric. For. Meteorol. 149, 291–302. https://doi. org/10.1016/j.agrformet.2008.08.011.

Helbig, M., Wischnewski, K., Gosselin, G.H., et al., 2016. Addressing a systematic bias in carbon dioxide flux measurements with the EC150 and the IRGASON open-path gas analyzers. Agric. For. Meteorol. 228–229, 349–359. https://doi.org/10.1016/j. agrformet.2016.07.018.

Horst, T., 1997. A simple formula for attenuation of eddy fluxes measured with firstorder-response scalar sensors. Bound. Layer Meteorol. 82, 219–233. https://doi.org/ 10.1023/A:1000229130034.

Horst, T.W., 2000. On frequency response corrections for eddy covariance flux measurements. Bound. Layer Meteorol. 94, 517–520. https://doi.org/10.1023/ A:1002427517744.

Horst, T.W., Lenschow, D.H., 2009. Attenuation of scalar fluxes measured with spatiallydisplaced sensors. Bound. Layer Meteorol. 130, 275–300. https://doi.org/10.1007/ s10546-008-9348-0.

Horst, T.W., Semmer, S.R., Maclean, G., 2015. Correction of a non-orthogonal, threecomponent sonic anemometer for flow distortion by transducer shadowing. Bound. Layer Meteorol. 155, 371–395. https://doi.org/10.1007/s10546-015-0010-3.

Horst, T.W., Vogt, R., Oncley, S.P., 2016. Measurements of flow distortion within the IRGASON integrated sonic anemometer and CO 2 /H 2 O gas analyzer. Bound. Layer Meteorol. 160. https://doi.org/10.1007/s10546-015-0123-8.

Huq, S., De Roo, F., Foken, T., Mauder, M., 2017. Evaluation of probe-induced flow distortion of campbell CSAT3 sonic anemometers by numerical simulation. Bound. Layer Meteorol. 165, 9–28. https://doi.org/10.1007/s10546-017-0264-z.

Ibrom, A., Dellwik, E., Flyvbjerg, H., et al., 2007a. Strong low-pass filtering effects on water vapour flux measurements with closed-path eddy correlation systems. Agric. For. Meteorol. 147, 140–156. https://doi.org/10.1016/j.agrformet.2007.07.007.

Ibrom, A., Dellwik, E., Larsen, S.E., Pilegaard, K., 2007b. On the use of the WebbPearman-Leuning theory for closed-path eddy correlation measurements. Tellus Ser. B Chem. Phys. Meteorol. 59, 937–946. https://doi.org/10.1111/j.1600-0889.2007. 00311.x.

Kaimal, J.C., Finnigan, J.J., 1994. Atmospheric Boundary Layer Flows: Their Structure and Measurement.

Kaimal, J.C., Wyngaard, J.C., Izumi, Y., Coté, O.R., 1972. Spectral characteristics of surface-layer turbulence. Q. J. R. Meteorol. Soc. 98, 563–589. https://doi.org/10. 1002/qj.49709841707.

Lee, X., Black, T.A., 1994. Relating eddy correlation sensible heat flux to horizontal sensor separation in the unstable atmospheric surface layer. J. Geophys. Res. 99, 18545. https://doi.org/10.1029/94JD00942.

Lenschow, D.H., Raupach, M.R., 1991. The attenuation of fluctuations in scalar concentrations through sampling tubes. J. Geophys. Res. 96, 15259. https://doi.org/10. 1029/91JD01437.

Leuning, R., Judd, M.J., 1996. The relative merits of open- and closed-path analysers for measurement of eddy fluxes. Glob. Change Biol. 2, 241–253. https://doi.org/10. 1111/j.1365-2486.1996.tb00076.x.

Leuning, R., King, K.M., 1992. Comparison of eddy-covariance measurements of CO2 fluxes by open- and closed-path CO2 analysers. Bound. Layer Meteorol. 59, 297–311. https://doi.org/10.1007/BF00119818.

Leuning, R., Moncrieff, J., 1990. Eddy-covariance CO2 flux measurements using openand closed-path CO2 analysers: corrections for analyser water vapour sensitivity and damping of fluctuations in air sampling tubes. Bound. Layer Meteorol. 53, 63–76. https://doi.org/10.1007/BF00122463.

Ma, J., Zha, T., Jia, X., et al., 2017. An eddy-covariance system with an innovative vortex intake for measuring carbon dioxide and water fluxes of ecosystems. Atmos. Meas. Tech. 10, 1259–1267. https://doi.org/10.5194/amt-10-1259-2017.

Mammarella, I., Launiainen, S., Gronholm, T., et al., 2009. Relative humidity effect on the high-frequency attenuation of water vapor flux measured by a closed-path eddy covariance system. J. Atmos. Ocean Technol. 26, 1856–1866. https://doi.org/10. 1175/2009JTECHA1179.1.

Massman, W.J., 2000. A simple method for estimating frequency response corrections for eddy covariance systems. Agric. For. Meteorol. 104, 185–198. https://doi.org/10. 1016/S0168-1923(00)00164-7.

Massman, W.J., 2001. Reply to comment by Rannik on “A simple method for estimating frequency response corrections for eddy covariance systems”. Agric. For. Meteorol. 107, 247–251. https://doi.org/10.1016/S0168-1923(00)00237-9.

Massman, W., Clement, R., 2005. Uncertainty in eddy covariance flux estimates resulting from spectral attenuation. Handb. Micrometeorol. 29, 67–99. https://doi.org/10. 1007/1-4020-2265-4_4.

Massman, W.J., Ibrom, A., 2008. Attenuation of concentration fluctuations of water vapor and other trace gases in turbulent tube flow. Atmos. Chem. Phys. 8, 6245–6259. https://doi.org/10.5194/acpd-8-9819-2008.

Mauder, M., Foken, T., 2006. Impact of post-field data processing on eddy covariance flux estimates and energy balance closure. Meteorol Zeitschrift 15, 597–609. https://doi. org/10.1127/0941-2948/2006/0167.

Mauder, M., Zeeman, M.J., 2018. Field intercomparison of prevailing sonic anemometers. Atmos. Meas. Tech. 11, 249–263. https://doi.org/10.5194/amt-11-249-2018.

Metzger, S., Burba, G., Burns, S.P., et al., 2016. Optimization of an enclosed gas analyzer sampling system for measuring eddy covariance fluxes of H2O and CO2. Atmos. Meas. Tech. 9, 1341–1359. https://doi.org/10.5194/amt-9-1341-2016.

Moncrieff, J.B., Massheder, J.M., de Bruin, H., et al., 1997. A system to measure surface fluxes of momentum, sensible heat, water vapour and carbon dioxide. J. Hydrol. 188–189, 589–611. https://doi.org/10.1016/S0022-1694(96)03194-0.

Moore, C.J., 1986. Frequency response correctionsfor eddy correlation systems. Bound. Layer Meteorol. 37, 17–35. https://doi.org/10.1007/BF00122754.

Nakai, T., Shimoyama, K., 2012. Ultrasonic anemometer angle of attack errors under turbulent conditions. Agric. For. Meteorol. 162–163, 14–26. https://doi.org/10. 1016/j.agrformet.2012.04.004.

Nakai, T., Van Der Molen, M.K., Gash, J.H.C., Kodama, Y., 2006. Correction of sonic anemometer angle of attack errors. Agric. For. Meteorol. 136, 19–30. https://doi.org/ 10.1016/j.agrformet.2006.01.006.

Nakai, T., Iwata, H., Harazono, Y., 2011. Importance of mixing ratio for a long-term CO2 flux measurement with a closed-path system. Tellus Ser. B Chem. Phys. Meteorol. 63, 302–308. https://doi.org/10.1111/j.1600-0889.2011.00538.x.

Nordbo, A., Katul, G., 2013. A wavelet-based correction method for eddy-covariance high-frequency losses in scalar concentration measurements. Bound. Layer Meteorol. 146, 81–102. https://doi.org/10.1007/s10546-012-9759-9.

Novick, K.A., Walker, J., Chan, W.S., et al., 2013. Eddy covariance measurements with a new fast-response, enclosed-path analyzer: spectral characteristics and cross-system comparisons. Agric. For. Meteorol. 181, 17–32. https://doi.org/10.1016/j.agrformet. 2013.06.020.

Pastorello, G., Papale, D., Chu, H., et al., 2017. A new data set to keep a sharper eye on land-air exchanges. Eos (Washington DC) 1–6. https://doi.org/ 10.1029/ 2017EO071597.

Runkle, B.R.K., Wille, C., Gažovič, M., Kutzbach, L., 2012. Attenuation correction procedures for water vapour fluxes from closed-path eddy-covariance systems. Bound. Layer Meteorol. 142, 401–423. https://doi.org/10.1007/s10546-011-9689-y.

Ruppert, J., Thomas, C., Foken, T., 2006. Scalar similarity for relaxed eddy accumulation methods. Bound. Layer Meteorol. 120, 39–63. https://doi.org/10.1007/s10546-005- 9043-3.

Sargent, S., 2015. Damping Temperature Fluctuations in the EC155 Intake Tube. Logan, UT. .

Schmidt, A., Hanson, C., Stephen Chan, W., Law, B.E., 2012. Empirical assessment of uncertainties of meteorological parameters and turbulent fluxes in the AmeriFlux network. J. Geophys. Res. Biogeosci. 117. https://doi.org/10.1029/2012JG002100.

Stull, R.B. (Ed.), 1988. An Introduction to Boundary Layer Meteorology. Springer, Netherlands, Dordrecht.

Su, H.B., Schmid, H.P., Grimmond, C.S.B., et al., 2004. Spectral characteristics and correction of long-term eddy-covariance measurements over two mixed hardwood forests in non-flat terrain. Bound. Layer Meteorol. 110, 213–253. https://doi.org/10. 1023/A:1026099523505.

Ueyama, M., Hirata, R., Mano, M., et al., 2012. Influences of various calculation options on heat, water and carbon fluxes determined by open- and closed-path eddy covariance methods. Tellus B 64, 19048. https://doi.org/10.3402/tellusb.v64i0.19048.

Wang, L., Lee, X., Wang, W., et al., 2017. A meta-analysis of open-path eddy covariance observations of apparent CO2flux in cold conditions in FLUXNET. J. Atmos. Ocean Technol. 34, 2475–2487. https://doi.org/10.1175/JTECH-D-17-0085.1.

Webb, E., Pearman, G., Leuning, R., 1980. Correction of flux measurements for density effects due to heat and water vapour transfer. Q. J. R. Meteorol. Soc. 106, 85–100. https://doi.org/10.1002/qj.49710644707.

Wyngaard, J.C., 1981. The effects of probe-induced flow distortion on atmospheric turbulence measurements. J. Appl. Meteorol. 20, 784–794. https://doi.org/10.1175/ 1520-0450(1981)0202.0.CO;2.

Wyngaard, J.C., 1988. Flow-distortion effects on scalar flux measurements in the surface layer: implications for sensor design. Bound. Layer Meteorol. 42, 19–26. https://doi. org/10.1007/BF00119872.

Zhang, J., Lee, X., Song, G., Han, S., 2011. Pressure correction to the long-term measurement of carbon dioxide flux. Agric. For. Meteorol. 151, 70–77. https://doi.org/ 10.1016/j.agrformet.2010.09.004.